In Vivo Quantification of Calcitonin Gene-Related Peptide Receptor Occupancy by Telcagepant in Rhesus Monkey and Human Brain Using the Positron Emission Tomography Tracer [11C]MK-4232

Eric D. Hostetler, Aniket D. Joshi, Sandra Sanabria-Bohórquez, Hong Fan, Zhizhen Zeng, Mona Purcell, Liza Gantert, Kerry Riffel, Mangay Williams, Stacey O'Malley, Patricia Miller, Harold G. Selnick, Steven N. Gallicchio, Ian M. Bell, Christopher A. Salvatore, Stefanie A. Kane, Chi-Chung Li, Richard J. Hargreaves, Tjibbe de Groot, Guy Bormans, Anne Van Hecken, Inge Derdelinckx, Jan de Hoon, Tom Reynders, Ruben Declercq, Inge De Lepeleire, W. P. Kennedy, Rebecca Blanchard, Eugene E. Marcantonio, Cyrille Sur, Jacquelynn J. Cook, Koen Van Laere, and Jeffrey L. Evelhoch

Merck Research Laboratories, West Point, Pennsylvania (E.D.H., A.D.J., S.S.-B., H.F., Z.Z., M.P., L.G., K.R., M.W., S.O., P.M. H.G.S., S.N.G., I.M.B., C.A.S., S.A.K., C.-C.L., R.J.H., C.S., J.J.C., J.L.E.); Division of Nuclear Medicine, University Hospital and KU Leuven, Leuven, Belgium (T.d.G., K.V.L.); Lab Radiopharmacy KU Leuven, Leuven, Belgium (G.B.); Merck Sharp and Dohme, Brussels, Belgium (T.R., R.D., I.D.L.); Merck Clinical Pharmacology, Upper Gwynedd, Pennsylvania (W.P.K., R.B.); Merck Clinical Pharmacology, Kenilworth, New Jersey (E.E.M.); and Center for Clinical Pharmacology, University Hospital and KU Leuven, Leuven, Belgium (A.v.H., I.D., J.d.H.)

Received May 17, 2013; accepted August 22, 2013

ABSTRACT

Calcitonin gene-related peptide (CGRP) is a potent neuropeptide whose agonist interaction with the CGRP receptor (CGRP-R) in the periphery promotes vasodilation, neurogenic inflammation and trigeminovascular sensory activation. This process is implicated in the cause of migraine headaches, and CGRP-R antagonists in clinical development have proven effective in treating migraine-related pain in humans. CGRP-R is expressed on blood vessel smooth muscle and sensory trigeminal neurons and fibers in the periphery as well as in the central nervous system. However, it is not clear what role the inhibition of central CGRP-R plays in migraine pain relief. To this end, the CGRP-R positron emission tomography (PET) tracer [11C]MK-4232 (2-[(8R)-8-(3,5-difluorophenyl)-6,8-[6-11C]dimethyl-10-oxo-6,9-diazaspiro[4.5]decan-9-yl]-N-[(2R)-2′-oxospiro[1,3-dihydroindene-2,3′-1H-pyrrolo[2,3-b]pyridine]-5-yl]acetamide) was discovered and developed for use in clinical PET studies. In rhesus monkeys and humans, [11C]MK-4232 displayed rapid brain uptake and a regional brain distribution consistent with the known distribution of CGRP-R. Monkey PET studies with [11C]MK-4232 after intravenous dosing with CGRP-R antagonists validated the ability of [11C]MK-4232 to detect changes in CGRP-R occupancy in proportion to drug plasma concentration. Application of [11C]MK-4232 in human PET studies revealed that telcagepant achieved only low receptor occupancy at an efficacious dose (140 mg PO). Therefore, it is unlikely that antagonism of central CGRP-R is required for migraine efficacy. However, it is not known whether high central CGRP-R antagonism may provide additional therapeutic benefit.

Introduction

Calcitonin gene-related peptide (CGRP) is a potent vasodilator and sensory neuropeptide that is believed to play a key role in the pathophysiology of migraine (Salvatore and Kane, 2011). The CGRP receptor (CGRP-R) is a heterodimeric complex,

ABBREVIATIONS: 2D, two-dimensional; 3D, three-dimensional; AMY, amylin; BBB, blood–brain barrier; CGRP, calcitonin gene-related peptide; CGRPA2, *N*-((1*R*)-1-(3,5-difluorophenyl)ethyl)-1,4-dimethyl-*N*-(2-oxo-2-(((2R)-2′-oxo-1,1′,2′,3-tetrahydrospiro[indene-2,3′-pyrrolo[2,3-b]pyridin]-5-yl)amino)ethyl)piperidine-4-carboxamide; CGRP-R, CGRP receptor; CLR, calcitonin receptor-like receptor; CNS, central nervous system; CTR, calcitonin receptor; E_{max}, maximal effective response; HPLC, high-performance liquid chromatography; K_d, dissociation constant; K_i, inhibition constant; MK-3207, 2-[(8*R*)-8-(3,5-difluorophenyl)-10-oxo-6,9-diazaspiro[4.5]dec-9-yl]-*N*-[(2*R*)-2′-oxo-1,1′,2′,3-tetrahydrospiro[indene-2,3′-pyrrolo[2,3-b]pyridin]-5-yl]acetamide; MK-4232, 2-[(8*R*)-8-(3,5-difluorophenyl)-6,8-dimethyl-10-oxo-6,9-diazaspiro[4.5]dec-9-yl]-*N*-[(2*R*)-2′-oxo-1,1′,2′,3-tetrahydrospiro[indene-2,3′-pyrrolo[2,3-b]pyridin]-5-yl]acetamide; MRI, magnetic resonance imaging; PET, positron emission tomography; P-gp, P-glycoprotein; RAMP, receptor activity-modifying protein; RO, receptor occupancy; SUV, standardized uptake value; TAC, time-activity curve; T-RT, test-retest; V_T, total volume of distribution.

composed of the calcitonin receptor-like receptor (CLR) and receptor activity-modifying protein-1 (RAMP1). CLR is a classic G-protein–linked receptor that is coupled through adenylyl cyclase. CGRP-Rs are expressed in the central nervous system (CNS), particularly in the brainstem and cerebellum as well as in the periphery on vascular smooth muscle cells. CGRP levels in the cranial circulation have been shown to increase during a migraine attack and CGRP itself has been shown to trigger migraine headache with concomitant dilation of the middle meningeal artery, a branch of the maxillary artery (Asghar et al., 2011). However, a recent study has contradicted these findings, suggesting that there is no dilation of extracranial arteries in migraine and the cause of migraine thus may be mediated by CNS mechanisms (Amin et al., 2013). Therefore, it is not clear whether CGRP-R antagonists are effective by antagonism of CGRP-R in the peripheral trigeminovascular system, or whether antagonism of central CGRP-R is a component of efficacy.

Telcagepant (Fig. 1) is a potent, selective CGRP-R antagonist (Paone et al., 2007), and clinical efficacy studies have established that telcagepant is effective in the treatment of acute migraine pain (Ho et al., 2008). Positron emission tomography (PET) is a technology that can noninvasively quantify relationships between the levels of drug administered and its receptor occupancy (RO) in central compartments (Matthews et al., 2012). Since the relationship between the efficacy of CGRP-R antagonists in migraine treatment and the extent of central CGRP RO is unknown, we sought to discover a CGRP-R PET tracer to quantify the level of central CGRP RO achieved by efficacious doses of telcagepant. This knowledge could support dose selection for CGRP-R antagonists in development and inform on the need for CNS penetration for a next generation of CGRP-R antagonists.

There are no published reports of a PET tracer for in vivo quantification of central CGRP-R. Herein, the characterization of the CGRP PET tracer $[^{11}C]$MK-4232 (2-[(8R)-8-(3,5-difluorophenyl)-6,8-dimethyl-10-oxo-6,9-diazaspiro[4.5]decan-9-yl]-N-[(2R)-2′-oxospiro[1,3-dihydroindene-2,3′-1H-pyrrolo[2,3-b]pyridine]-5-yl]acetamide) in rhesus monkey and human PET studies is described, including $[^{11}C]$MK-4232 PET RO studies with telcagepant in the human brain. In addition, PET studies with $[^{11}C]$CGRPA2 [N-((1R)-1-(3,5-difluorophenyl)ethyl)-1,4-[4-$^{11}C]$dimethyl-N-(2-oxo-2-(((2R)-2′-oxo-1,1′,2′,3-tetrahydrospiro[indene-2,3′-pyrrolo[2,3-b]pyridin]-5-yl)amino)ethyl)piperidine-4-carboxamide], a non-brain-penetrant CGRP-R antagonist, were performed to investigate the potential contribution of vascular CGRP-R to the brain CGRP-R PET signal.

Materials and Methods

$[^{11}C]CO_2$ was produced by Siemens Molecular Imaging Biomarker Solutions, Inc. (North Wales, PA). The $[^{11}C]CO_2$ was converted to $[^{11}C]$methyl triflate using a TRACERlab FXc (GE Healthcare, Wauwatosa, WI). Telcagepant, MK-3207 (2-[(8R)-8-(3,5-difluorophenyl)-10-oxo-6,9-diazaspiro[4.5]dec-9-yl]-N-[(2R)-2′-oxo-1,1′,2′,3-tetrahydrospiro[indene-2,3′-pyrrolo[2,3-b]pyridin]-5-yl]acetamide), MK-4232, N-desmethyl MK-4232, CGRPA2, and N-desmethyl CGRPA2 were prepared at Merck Research Laboratories (West Point, PA) according to published methods (Paone et al., 2007; Bell et al., 2010, 2013). Radiochemical procedures were performed remotely in a lead hot cell using a modified 233XL liquid handler (Gilson, Inc., Middleton, WI) (Hostetler et al., 2001). The PET tracer identity, radiochemical purity, and specific activity were determined by evaluation on a Waters 600E high-performance liquid chromatography (HPLC) system equipped with a Waters 996 UV detector (Waters, Milford, MA) and a FlowCount photodiode radiodetector (Bioscan Inc., Washington, DC). A Waters XTerra C18 column (4.6 × 150 mm, 5 μm) with a mobile phase of acetonitrile (solvent A) and 95:5 MeCN/H_2O (0.1% trifluoroacetic acid) (solvent B) at 1 ml/min was used with a 15-minute linear gradient of 20:80 A/B to 90:10 A/B. The identity of the radioligand was determined by an independent coinjection with unlabeled reference compound. Radiochemical purity was determined by calculating the percent radioactivity attributed to isolated peak in the radioactive HPLC trace after integration of all radioactive peaks. The specific activity (GBq/μmol)
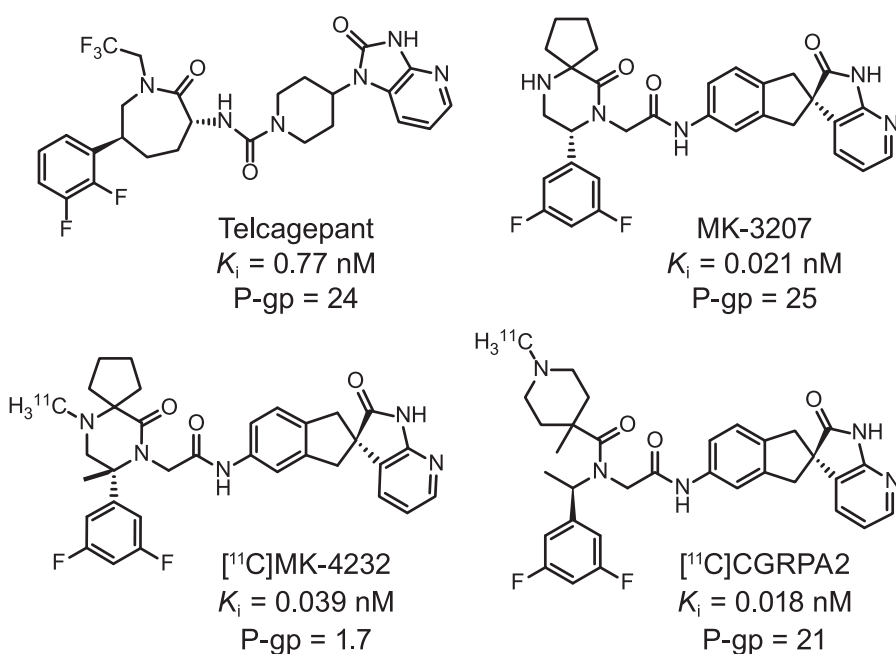

Telcagepant
K_i = 0.77 nM
P-gp = 24

MK-3207
K_i = 0.021 nM
P-gp = 25

$[^{11}C]$MK-4232
K_i = 0.039 nM
P-gp = 1.7

$[^{11}C]$CGRPA2
K_i = 0.018 nM
P-gp = 21

Fig. 1. Structure and selected properties of the CGRP-R antagonists telcagepant, MK-3207, $[^{11}C]$MK-4232, and $[^{11}C]$CGRPA2.

of the radioligand was determined by withdrawing an aliquot (0.5–1.5 ml) of the tracer, determining the amount of radioactivity in a dose calibrator, and correcting for decay from end of synthesis. The aliquot was evaluated by HPLC and the UV response was compared against a calibration curve that was prepared with the unlabeled reference standard to determine the mass associated with the decay-corrected radioactivity of the injected aliquot.

In Vitro Binding Studies

The inhibition constant (K_i) for inhibition of [^{125}I]CGRP binding was determined as previously described using membranes from human embryonic kidney 293 cells stably expressing human CGRP (Salvatore et al., 2008). MK-4232 binding to CLR and calcitonin receptor (CTR) heterodimers CLR/RAMP3, CTR/RAMP1, and CTR/RAMP3 was determined as previously described (Salvatore et al., 2010). In vitro binding studies with [^{3}H]MK-4232 in rhesus monkey (female donor) and human (male donor) brain cerebellum homogenate were performed analogous to previously reported procedures (Hamill et al., 2009).

Lipophilicity Measurements

The log D of MK-4232 was determined by partitioning the compound between octanol and phosphate buffer at pH 7.4 and measuring the concentration of MK-4232 in each layer (Dohta et al., 2007).

Transport in P-Glycoprotein–Transfected Cell Lines

The P-glycoprotein (P-gp) transport ratio (i.e., the ratio of permeabilities across each direction of the cell monolayer) for each compound was evaluated across monolayers of porcine renal epithelial cells overexpressing human P-gp (Yamazaki et al., 2001). Verapamil, a known P-gp substrate, was evaluated as a positive control.

Autoradiography

Autoradiography with [^{3}H]MK-4232 in rhesus monkey (male donor) and human (female donor) brain slices was performed similar to previously reported methods (Hamill et al., 2009). Brain slices were incubated at room temperature with [^{3}H]MK-4232 (0.1 nM).

Preclinical PET Studies

Animals. All monkey PET imaging studies were conducted under the guiding principles of the American Physiologic Society and the National Institutes of Health (NIH) *Guide for the Care and Use of Laboratory Animals* (NIH publication no. 85-23, revised 1996) and were approved by the West Point Institutional Animal Care and Use Committee at Merck Research Laboratories. Rhesus monkeys (male, approximately 10 kg, $n = 6$) were initially sedated with ketamine (10 mg/kg i.m.) and then induced with propofol (5 mg/kg i.v.), intubated, and respired with medical-grade air at approximately 10 ml per breath per kilogram and 20 respirations per minute. The anesthesia was maintained with propofol (0.4 mg·kg^{-1}·min^{-1}) for the duration of the study. Body temperature was maintained with circulating water heating pads, and temperature, oxygen saturation, and end-tidal CO_2 were monitored for the duration of the study.

Preparation of [^{11}C]MK-4232 and [^{11}C]CGRPA2. [^{11}C]MK-4232 was prepared by distillation of [^{11}C]methyl triflate (11.1 GBq) into a solution of *N*-desmethyl MK-4232 (0.5 mg, 0.9 μmol) in acetone (0.3 ml) at room temperature. After 1 minute, the reaction was diluted with 10 mM disodium phosphate (0.25 ml) and purified by semi-preparative HPLC (Gemini C18 column, 10 × 150 mm, 5 μm; Phenomenex, Torrance, CA) using a mobile phase of 60:40 ethanol/5 mM sodium citrate at a flow of 3 ml/min. The peak corresponding to [^{11}C]MK-4232 (retention time of approximately 8 minutes) was collected, diluted with saline, and transferred to a sterile capped vial to provide [^{11}C]MK-4232 with a radiochemical purity >97% and specific activity >37 GBq/μmol.

With the exception of using *N*-desmethyl CGRPA2 as the precursor, [^{11}C]CGRPA2 was prepared using methods analogous to those used for [^{11}C]MK-4232.

Imaging Procedure. PET scans were performed on an ECAT EXACT HR+ (Siemens Healthcare, Knoxville, TN) in three-dimensional (3D) mode; transmission data for attenuation correction were acquired in two-dimensional (2D) mode before injection of the radiopharmaceutical. Dynamic emission scans were performed for 120 minutes after bolus intravenous injection of [^{11}C]MK-4232 or [^{11}C]CGRPA2 (approximately 185 MBq). Data were reconstructed using a 3D ordered-subset expectation maximization iterative algorithm with 6 iterations and 16 subsets and an all-pass ramp filter. Animals were scanned on a Siemens Trio 3T magnet to obtain magnetic resonance images.

For RO PET studies, a CGRP-R antagonist (MK-4232, MK-3207, or telcagepant) was administered as an intravenous bolus plus constant infusion (in 10:40:50 ethanol/PEG400/H$_2$O) starting 60 minutes before tracer injection with the infusion maintained throughout the PET scan. For some studies, telcagepant was administered orally via oral gavage (in 1:1 Imwitor 742/polysorbate 80) 24 hours prior to tracer injection. For each PET study, [^{11}C]MK-4232 plasma concentrations were obtained from the measurement of total radioactivity in arterial plasma with correction for the fraction of intact tracer as determined by HPLC analysis. Plasma drug levels of telcagepant, MK-3207, or MK-4232 during the PET scan were determined from venous blood samples.

Image Analysis and Quantification. PET data were corrected for isotope decay, attenuation, scatter, and dead-time. For each animal, a PET template was obtained by averaging all of the frames in the dynamic acquisition under baseline conditions. Each animal's magnetic resonance imaging (MRI) scan and PET template were coregistered using SPM99 (http://www.fil.ion.ucl.ac.uk/spm). With the assistance of the MRI scan and the PET template, regions of interest were then drawn using the Montreal Neurologic Institute DISPLAY software. All subsequent PET images were coregistered to the PET template.

Tissue time-activity curves (TACs) were obtained by projecting the defined regions of interest onto all frames of the dynamic PET scans and were expressed as the standardized uptake value (SUV) by using the animal's weight and the corresponding tracer injected activity (Bq) (eq. 1):

$$TAC(SUV) = \frac{TAC(Bq/ml) \times Weight(kg) \times 1000(ml/kg)}{Tracer\ injected(Bq)} \quad (1)$$

Coregistration of PET scans to PET templates, extraction of TACs from dynamic scans, and all subsequent analyses were performed using in-house developed analysis software written in Matlab (The MathWorks, Inc., Natick, MA).

The TACs were fit using spectral analysis, a data-driven method, using the metabolite-corrected arterial input function to determine the total volume of distribution (V_T) (Cunningham and Jones, 1993). Percent test-retest (T-RT) variability of V_T was determined as follows (eq. 2):

$$T - RT(\%) = 100\% \times 2 \times \frac{|V_T(scan\ 1) - V_T(scan\ 2)|}{V_T(scan\ 1) + V_T(scan\ 2)} \quad (2)$$

RO was calculated using the Lassen plot (Cunningham et al., 2010). For each PET occupancy study, the estimated RO was associated with the average drug plasma levels during the PET scan. SigmaPlot (version 9.0; SYSTAT Software, San Jose, CA) was used to obtain the relationship between CGRP RO and plasma drug concentrations for MK-4232 and MK-3207 based on a two-parameter Hill equation ($E_{max} = 100\%$). The telcagepant data set lacked the range of PET occupancy data desired for a robust curve fit; therefore, a one-parameter Hill equation with the Hill coefficient fixed at 1.0 and $E_{max} = 100\%$ was used to describe the telcagepant plasma level/CGRP RO relationship.

Human PET Studies

Subjects. Healthy male volunteers participated in these studies ($n = 10$; age range, 21–49 years). Subjects were recruited through advertisements placed in a local newspaper and on a hospital website. Written informed consent was obtained before undergoing the PET study. These experiments conformed to the International Guidelines of Good Clinical Practice and the latest version of the Declaration of Helsinki for healthy volunteer studies, and were approved by the Ethics Committee of the University Hospitals of Leuven (Leuven, Belgium). The safety and tolerability of [11C]MK-4232 was assessed throughout the study by monitoring subjects for clinical adverse experiences. Physical examinations, vital sign measurements, 12-lead electrocardiograms, and laboratory safety tests (hematology, chemistry, and urinalysis) were performed at specified intervals to detect any medically meaningful effects of the tracer on physiology.

Preparation of [11C]MK-4232. Preparation of [11C]MK-4232 was similar to the procedure described for rhesus monkey PET studies with slight modifications. The reaction mixture was diluted with aqueous disodium phosphate (10 mM) and purified by isocratic semipreparative HPLC using an eluent of 55% ethanol, 45% 10 mM disodium phosphate at a flow rate of 2 ml/min. The radioactive peak corresponding to [11C]MK-4232 was collected, diluted, and passed through a sterile filter into a sterile vial to provide a sterile, pyrogen-free solution of [11C]MK-4232 in 10% ethanol, 1% Captisol, 10 mM sodium phosphate, 0.9% sodium chloride, pH 7.4. The formulated [11C]MK-4232 had a radiochemical purity $\geq$95% and the mass of unlabeled MK-4232 administered was $\leq$6 μg per tracer administration for all PET occupancy studies.

Imaging Procedure. PET scans were performed on a Hi-Rez Biograph 16 scanner (Siemens Healthcare). Prior to scanning, a venous cannula was inserted for tracer injection and, for occupancy studies, blood sampling for determination of telcagepant plasma levels. A radial artery cannula was placed under local anesthesia for blood sampling to determine the arterial plasma concentration of radioactivity due to [11C]MK-4232. The head was restrained to reduce movement artifacts during the scan. After positioning of the subject in the scanner, approximately 300 MBq of [11C]MK-4232 was injected intravenously, simultaneously starting a 90- or 120-minute dynamic emission PET scan. Data were reconstructed using a 3D ordered-subset expectation maximization iterative reconstruction with five iterations and eight subsets and a postsmoothing with a 3D Gaussian filter (5 mm full width at half maximum). In addition to the PET scans, all subjects underwent a volumetric T1-weighted MRI scan with $1\times1\times1$ mm voxel size.

Six healthy male subjects received two baseline PET scans with [11C]MK-4232 (intravenously; bolus or 5-minute infusion) on the same day or on consecutive days to determine the T-RT variability of tracer V_T. For PET occupancy studies ($n = 6$), each subject was given an oral dose of telcagepant (140 or 1120 mg). The PET scan was initiated either 2 hours (for the 140 mg dose) or 3 hours (for the 1120 mg dose) postdose. For all studies, arterial blood samples (2 ml) were withdrawn manually throughout the PET scan to measure the [11C]MK-4232 arterial input function curve. The samples were centrifuged and the resulting plasma was counted in a gamma counter. Additional arterial samples (5 ml) were taken for measuring the fraction of unchanged [11C]MK-4232 in plasma. After each 5-ml sample, the line was flushed with heparinized saline. For background, a 1.5-ml blood sample was taken prior to radiotracer injection. The measured [11C]MK-4232 fractions were fit to a monoexponential function: $f(t) = a_1e^{-bt}+a_2$. This function was used to correct the total plasma radioactivity for radiolabeled metabolites, thus providing the [11C]MK-4232 arterial input function needed for tracer kinetic modeling and quantification of CGRP-R availability.

Image Analysis and Quantification. PET data processing, TAC generation, TAC fitting, and RO estimation were performed as described for the rhesus monkey PET studies. For each PET occupancy study, the average plasma concentration of telcagepant during the PET study was associated with the RO determined from the PET study.

Results

Affinity and Specificity

MK-4232 demonstrated high binding affinity (K_i = 0.046 nM) for the recombinant human CGRP-R. MK-4232 is selective for the CGRP-R (CLR/RAMP1) relative to the adrenomedullin 2 receptor (CLR/RAMP3) (K_i = 211 nM). MK-4232 displays high affinity for the related human amylin 1 (AMY$_1$; CTR/RAMP1) receptor (K_i = 0.6 nM), and is selective versus the human amylin 3 (AMY$_3$; CTR/RAMP3) receptor (K_i = 212 nM).

In Vitro Tissue Binding Studies

[3H]MK-4232 exhibits specific binding in vitro in rhesus monkey and human brain (Figs. 2 and 3) and the anatomic localization of [3H]MK-4232 binding sites are consistent with the known distribution of the CGRP-R (Tschopp et al., 1985; Inagaki et al., 1986; Salvatore et al., 2010). The cerebellum and substantia nigra showed the highest binding density, and the meninges, brainstem, and hippocampus showed moderate binding density. Low binding density was observed throughout the remainder of the cerebral gray matter. In vitro saturation binding studies with [3H]MK-4232 in rhesus monkey and human cerebellum homogenates showed that MK-4232 binds with high affinity to a single, saturable binding site in rhesus monkey and human cerebellum (Table 1).

Rhesus Monkey PET Studies

Baseline PET studies with [11C]MK-4232 in rhesus monkeys revealed rapid tracer distribution into the brain that did not clear appreciably from the brain during the duration of the PET scan (Fig. 4). [11C]MK-4232 concentration was highest in the cerebellum and brainstem, moderate in all other gray matter regions, and lowest in white matter (Fig. 5), consistent with the known distribution of CGRP-R. [11C]MK-4232 kinetics were described by spectral analysis, a data-driven
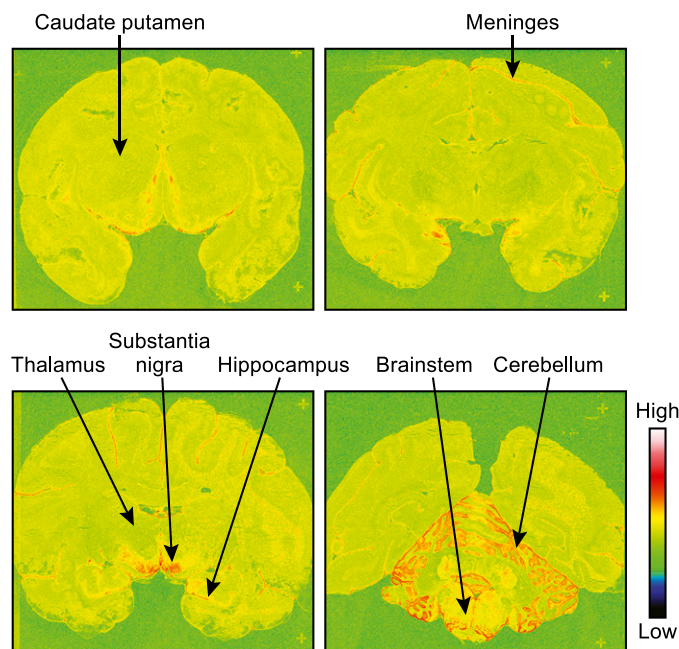

Fig. 2. [3H]MK-4232 in vitro autoradiography of rhesus monkey brain slices.
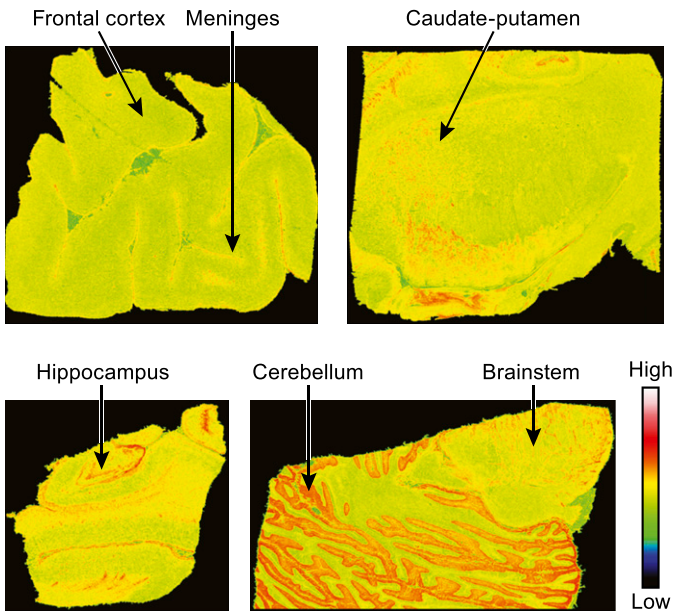
Fig. 3. [^{3}H]MK-4232 in vitro autoradiography of human brain slices.

method using the metabolite-corrected arterial input function (Cunningham and Jones, 1993). [^{11}C]MK-4232 V_T estimates were stable after 60 minutes of PET data. Repeat baseline scans with [^{11}C]MK-4232 in six monkeys showed intrasubject V_T variability of 4 ± 2% (Table 2).

Baseline PET studies with the potent CGRP-R antagonist [^{11}C]CGRPA2 in rhesus monkeys revealed no significant binding signal in the brain (Fig. 6). This result is consistent with the localization of CGRP-Rs in the brain and the inability of [^{11}C]CGRPA2 to access the brain due to P-gp susceptibility. In vitro, [^{3}H]CGRPA2 displays the same distribution and binding site density in monkey brain as does [^{3}H]MK-4232 (Zeng et al., 2009).

Initial rhesus monkey CGRP-R PET occupancy studies were conducted with unlabeled MK-4232 to characterize the utility of [^{11}C]MK-4232. As expected, increased plasma levels of MK-4232 were concomitant with increased CGRP-R occupancy as measured by [^{11}C]MK-4232 PET studies. Subsequent PET occupancy studies with two different CGRP-R antagonists, MK-3207 and telcagepant, confirmed the ability of [^{11}C]MK-4232 to differentiate the in vivo potency of CGRP-R antagonists (Fig. 7). The PET-determined Occ_{50} values for MK-4232, MK-3207, and telcagepant were 11 ± 3, 440 ± 130, and 5700 ± 1900 nM, respectively.

Human Baseline PET Studies with [^{11}C]MK-4232

Clinical safety data indicated that intravenous administration of [^{11}C]MK-4232 was generally safe and well tolerated. There were no adverse experiences related to the administration of [^{11}C]MK-4232.

TABLE 1
B_{max} and K_d values derived from the single-site curve-fit to [^{3}H]MK-4232 saturation binding in monkey and human cerebellum tissue homogenates

Tissue	B_{max}	K_d	B_{max}/K_d
	nM	nM	
Rhesus monkey cerebellum	23.9 ± 3.4	0.22 ± 0.04	113 ± 26
Human cerebellum	33.4 ± 1.0	0.27 ± 0.09	131 ± 39

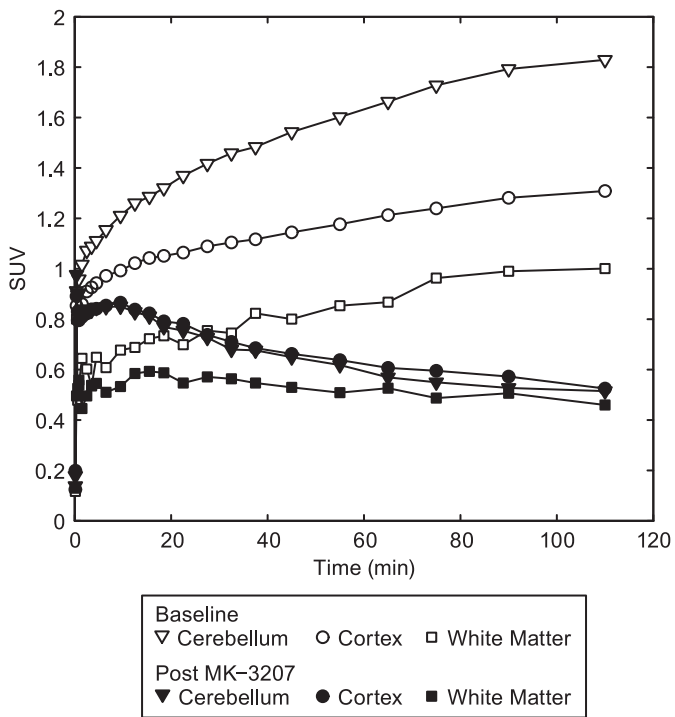Fig. 4. [^{11}C]MK-4232 TACs in rhesus monkey brain cerebellum (triangles), cortex (circles), and white matter (squares) at baseline (open symbols) and post–MK-3207 (filled symbols).

Baseline [^{11}C]MK-4232 distribution and kinetics in human brain were similar to those observed in monkey brain: rapid brain penetration followed by a slow increase in tracer distribution throughout all brain regions over the time period measured (Fig. 8). The highest tracer concentration was found in the cerebellum, with moderate levels of distribution throughout the rest of the gray matter. The tracer concentration in the white matter was lower than in gray matter, similar to that in rhesus monkeys and consistent with autoradiography with [^{3}H]MK-4232 in human brain tissue slices.

[^{11}C]MK-4232 V_T in humans was calculated using spectral analysis with the metabolite-corrected tracer arterial input function. Comparison of the cerebellum V_T using 60, 90, and 120 minutes of PET data revealed that V_T was stable after 60 minutes of PET data (data not shown). The average T-RT variability of baseline [^{11}C]MK-4232 V_T in the cerebellum was 6 ± 3% (n = 6 subjects) (Table 3).

Human CNS Occupancy by Telcagepant

Initial central RO PET studies with telcagepant were performed at a dose of 1120 mg. [^{11}C]MK-4232 was administered approximately 3 hours after the telcagepant dose to
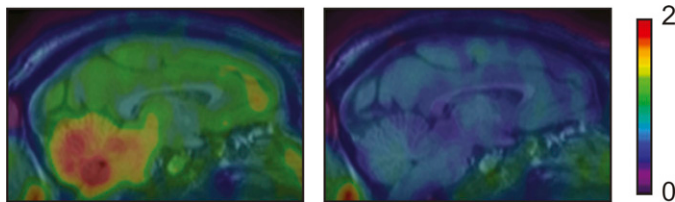

Fig. 5. Averaged (0–90 minutes) PET images (overlaid on MRI image) of [^{11}C]MK-4232 in rhesus monkeys at baseline (left image) and after MK-3207 administration (right image). Color scale is in SUV.

TABLE 2
Repeat measure of [^{11}C]MK-4232 baseline V_T in six rhesus monkeys

Monkey	V_T Baseline	V_T Baseline 2	T-RT
	ml/cm^3	ml/cm^3	%
A	13.5	13.7	1
B	12.7	13.5	5
C	11.1	11.4	3
D	14.6	15.1	4
E	13.2	13.5	3
F	14.5	13.4	8

coincide with T_{max} of the 1120 mg dose. RO was determined from a 90-minute PET scan. Tracer uptake was decreased in all regions relative to the baseline scan in the same subject (Figs. 8 and 9). A moderate RO (43–58%) was achieved by this high dose of telcagepant in three healthy volunteers (Table 4).

Additional RO studies were conducted at 140 mg telcagepant, a dose that has been shown to be effective for the treatment of a migraine attack (Ho et al., 2010). [^{11}C]MK-4232 was administered approximately 2 hours post-telcagepant to correspond with the primary efficacy pain freedom and pain relief endpoints in previous clinical studies. Tracer uptake in the brain did not decrease appreciably relative to the baseline scan in the same subject (Fig. 9). Kinetic modeling of the PET data revealed very low (≤10%) central CGRP RO in three subjects that underwent PET studies after a 140 mg dose of telcagepant (Table 4).

Discussion

[^{11}C]MK-4232 meets all of the basic in vitro criteria for a CNS PET tracer: high affinity (K_d = 0.27 nM in human brain tissue), moderate lipophilicity (log D = 3.38), good passive cell permeability (25×10^{-6} cm/s), and low susceptibility for P-gp (P-gp transport ratio = 1.7) (Patel and Gibson, 2008). In addition, [^{11}C]MK-4232 is synthesized utilizing a simple and reliable radiochemical reaction which provides the radio-tracer in good radiochemical yield and with high purity (>95%) and high specific activity (>37 GBq/μmol). These characteristics are critical for routine PET tracer production in a clinical setting.

Saturation binding studies with [^{3}H]MK-4232 in cerebellum tissue homogenate from rhesus monkey and human brain
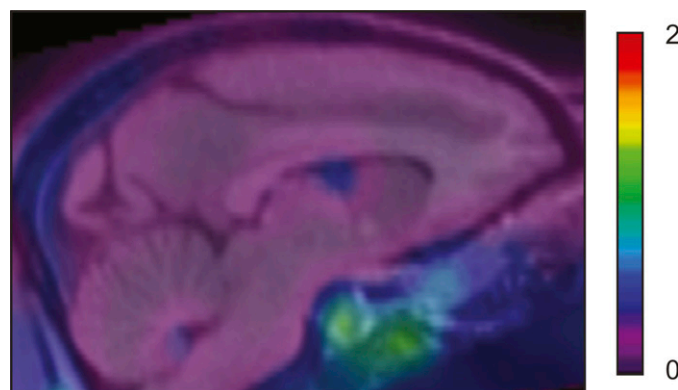

Fig. 6. Averaged (0–90 minutes) PET image (overlaid on MRI image) of [^{11}C]CGRPA2 in rhesus monkeys at baseline. Color scale is in SUV.
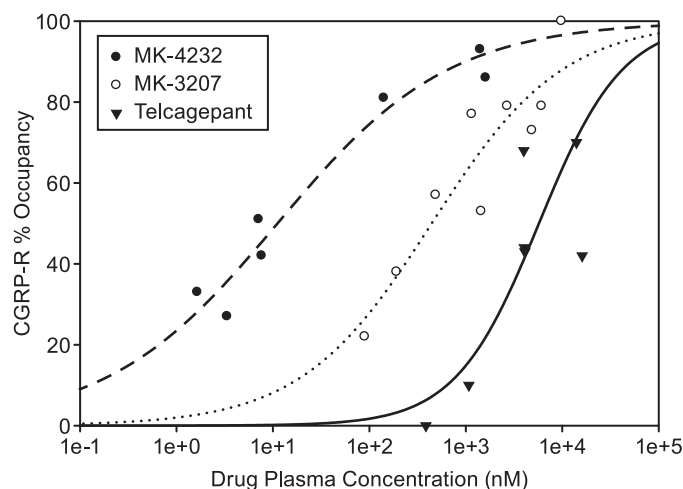

Fig. 7. Plot of drug plasma concentration versus CGRP RO for MK-4232 (filled circles), MK-3207 (open circles), and telcagepant (filled triangles) in rhesus monkeys as determined from PET studies occupancy studies using [^{11}C]MK-4232.

indicate that MK-4232 binds to a single site of similar density with identical affinity in the cerebellum of both species, indicating excellent selectivity for imaging CGRP-R. The B_{max}/K_d ratio observed in the cerebellum was similar in humans and rhesus monkeys. The in vivo signal from a PET tracer is expected to be directly proportional to its in vitro B_{max}/K_d ratio. Hence, [^{11}C]MK-4232 was predicted to provide a large specific signal in human cerebellum, comparable with the specific signal observed in the cerebellum of rhesus monkeys.

In vivo PET studies in rhesus monkeys show that [^{11}C]MK-4232 penetrates the blood–brain barrier (BBB) rapidly, with
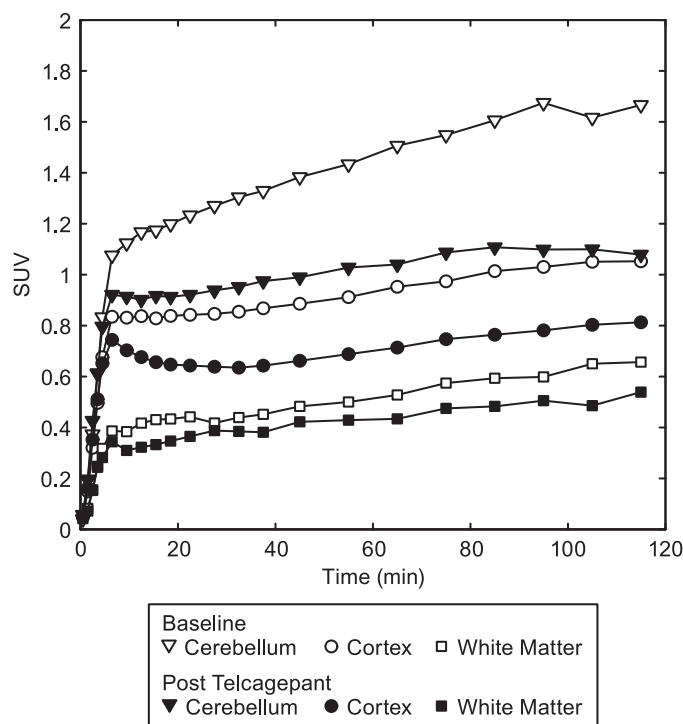

Fig. 8. [^{11}C]MK-4232 TACs in human brain cerebellum (triangles), cortex (circles), and white matter (squares) at baseline (open symbols) and post-telcagepant (1120 mg) (filled symbols).

TABLE 3
Repeat measure of [^{11}C]MK-4232 baseline V_T in six healthy human volunteers

Subject	V_T Baseline 1	V_T Baseline 2	T-RT
	ml/cm^3	ml/cm^3	%
1	10.3	10.8	5
2	11.0	11.8	7
3	13.4	13.5	1
4	12.3	13.1	7
5	13.4	14.7	9
6	11.9	10.9	9

a regional brain distribution consistent with in vitro autoradiography results and the known distribution of CGRP-R. The highest concentration of [^{11}C]MK-4232 is observed in the cerebellum. The exact role of CGRP-R localization in the cerebellum in not clear, but activation of cerebellar regions has been demonstrated by PET in patients during migraine attacks (Weiller et al., 1995; Bahra et al., 2001), and recent studies indicate that the cerebellum might have a role in nociception and migraine (Vincent and Hadjikhani, 2007; Borsook et al., 2008; Moulton et al., 2010). Spreading depression, cerebellar dysfunction, and familial hemiplegic migraine have also suggested a connection between the cerebellum and migraines. Moderate concentration of [^{11}C]MK-4232 was observed throughout the rest of the brain. Since the maximum resolution of the PET camera used in these studies is approximately 5 mm axially, tracer binding in regions with dimensional attributes smaller than the axial resolution of the camera is subject to partial volume effects; therefore, the tracer appears distributed over a larger volume than in reality. For [^{11}C]MK-4232, this phenomenon occurs with the tracer binding in the meninges, which is manifested as distribution in the cortex and other gray matter regions in which meninges are present. In vitro autoradiography, a technique of much higher resolution, is able to identify tracer binding in the area of the meninges (Figs. 2 and 3). However, autoradiography does not have sufficient resolution to identify the exact location of tracer distribution in the meninges (e.g., blood vessels, dura, arachnoid, or pia mater).

The localization of [^{11}C]MK-4232 displaceable binding in monkey brain was confirmed to be in the CNS gray matter, not in the brain vasculature, by evaluation of PET studies with the non-brain-penetrant CGRP-R PET tracer [^{11}C]CGRPA2. As a P-gp substrate, [^{11}C]CGRPA2 would only show a PET signal related to binding in the vasculature or distribution in other non-CNS organs. If CGRP-R were present in the brain vasculature in sufficient concentrations for imaging, a PET signal would have been observed with [^{11}C]CGRPA2. This provides evidence that the binding observed in PET studies with [^{11}C]MK-4232 is on the brain side of the BBB. However, this does not preclude the vasculature as the site of action for CGRP-R antagonists in migraine treatment. It only suggests

that the concentration of CGRP-Rs in the cerebral blood vessels are not of sufficient density to provide an imaging signal in a PET study with [^{11}C]CGRPA2. The brain uptake of [^{11}C]MK-4232 continued to rise over time after the initial rapid brain uptake. Formation of brain-penetrant radioactive metabolites may be a possible explanation for the increase of radioactivity in the brain over time. However, the tracer kinetics in the brain are reflective of [^{11}C]MK-4232 kinetics in plasma, which also typically rise slightly throughout the PET scan. In addition, the V_T values stabilize by 60 minutes, indicating that the tracer kinetics in the brain achieve steady state rapidly with respect to kinetics in plasma. Compartmental modeling of the tracer data suggests a low k_2 (efflux constant from brain to plasma), which may explain the slow tracer kinetics in the brain (Innis et al., 2007). Reassuringly, the tracer model accurately describes the tracer kinetics under both baseline and drug challenge conditions.

[^{11}C]MK-4232 was demonstrated to be useful for quantification of CGRP-R occupancy in rhesus monkeys. The average T-RT variability of [^{11}C]MK-4232 V_T at baseline was 4 ± 2% ($n = 6$ monkeys). This low baseline variability provides further confidence that if there are radiolabeled brain-penetrant metabolites, their levels are low and/or they are consistent from scan to scan. In addition, the low baseline variability suggests that [^{11}C]MK-4232 will be sufficiently sensitive to determine small changes in occupancy by CGRP-R antagonists. Further characterization of [^{11}C]MK-4232 in RO studies with MK-4232, MK-3207, and telcagepant confirmed this ability. Evaluation of the RO achieved by MK-4232 and MK-3207 at steady-state plasma levels revealed drug plasma/receptor occupancy relationships that were described by a two-parameter Hill equation as expected for a well behaved PET tracer (Fig. 7). Significantly, high plasma levels of MK-3207 demonstrated that it is possible to achieve complete displacement of [^{11}C]MK-4232 in vivo in all regions of rhesus monkey brain (Figs. 4 and 5).

It is also of interest that MK-3207, a P-gp substrate, blocked the [^{11}C]MK-4232 signal in the cortex (i.e., meninges) in concert with the [^{11}C]MK-4232 signal in the cerebellum. This provides further evidence that the CGRP-Rs visualized in the meninges in the [^{3}H]MK-4232 autoradiography studies and [^{11}C]MK-4232 PET studies are primarily on the brain side of the BBB. If the specific binding in the meninges were on the blood side of the BBB, a P-gp substrate such as MK-3207 would block tracer uptake in the cortex at lower plasma levels than those required to block tracer uptake in the cerebellum, where CGRP-Rs are predominantly localized in gray matter. However, evaluation of [^{11}C]MK-4232 PET data from occupancy studies with MK-3207 and telcagepant revealed changes in tracer binding in the cortex and cerebellum changed in concert. PET occupancy studies with CGRP-R antagonists telcagepant, MK-3207, and MK-4232 confirmed
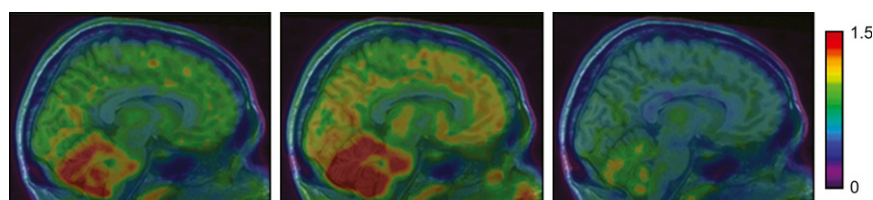
Fig. 9. [^{11}C]MK-4232 averaged PET images (overlaid on MR image) in human brain at baseline (left panel) and after 140 and 1120 mg telcagepant (center and right panels, respectively). Color scale is in SUV.

TABLE 4
CGRP RO by telcagepant (140 or 1120 mg PO) in human brain determined from [^{11}C]MK-4232 PET studies

Subject	Telcagepant Dose	Telcagepant Plasma Concentration	CGRP-R Occupancy
	mg	*μM*	*%*
1	1120	16.3 ± 1.84	43
7	1120	20.2 ± 3.93	48
8	1120	22.2 ± 4.43	58
9	140	0.254 ± 0.140	5
1	140	0.859 ± 0.305	10
10	140	0.424 ± 0.187	4

the ability of [^{11}C]MK-4232 to differentiate the in vivo potency of CGRP-R antagonists as expected (Occ$_{50}$: MK-4232 < MK-3207 < telcagepant) based on the combination of rank order of in vitro affinity for CGRP-R (K_i: MK-4232 ~ MK-3207 < < telcagepant) and susceptibility for the BBB efflux pump P-gp (P-gp efflux ratio: MK-4232 < < MK-3207 ~ telcagepant).

Human baseline PET studies with [^{11}C]MK-4232 showed tracer kinetics and distribution very similar to what was observed in rhesus monkey PET studies, with rapid tracer distribution into the brain that continued to increase slowly over the duration of the PET scan. T-RT variability of [^{11}C]MK-4232 V_T in cerebellum was low on average (6 ± 3%) in all six human subjects evaluated, suggesting that [^{11}C]MK-4232 will be sensitive to measurement of small changes in RO. The PET RO studies with 140 mg telcagepant were designed to emulate the timing of phase III clinical efficacy studies in migraineurs (Ho et al., 2010). This approach allowed for projection of the central CGRP RO achieved at the time of telcagepant efficacy measurement. Initial studies in healthy volunteers at a high dose of telcagepant (1120 mg) showed that significant central CGRP RO is achieved at supratherapeutic doses. However, at a lower, efficacious dose (140 mg) of telcagepant, very low RO (≤10%) was observed (Table 4). Orthosteric antagonist mechanisms typically require moderate to high RO to produce a pharmacodynamic effect resulting in efficacy (Grimwood and Hartig, 2009). Therefore, the very low occupancy achieved by an efficacious dose of telcagepant indicates that central occupancy of CGRP-R is not required for efficacy in migraineurs. However, it is possible that high central RO (e.g., >70%) may provide additional efficacy for migraineurs or for some other therapeutic indication. It is of note that the patient response rate in telcagepant efficacy studies was approximately 50%. One could speculate that some subjects may require more extensive, central antagonism of CGRP-R to achieve migraine relief. A therapeutic candidate with the ability to achieve higher CGRP RO at a well tolerated dose is needed to clinically test these hypotheses.

In conclusion, [^{11}C]MK-4232 is a suitable PET tracer for determination of CGRP-R occupancy in rhesus monkeys and healthy human volunteers. MK-3207 and telcagepant are potent CGRP-R antagonists that affect plasma concentration-dependent antagonism of CGRP-R in rhesus monkey brain as determined by [^{11}C]MK-4232 PET studies. In a limited number of human PET studies, high plasma concentrations of telcagepant (16–22 μM) resulted in moderate CGRP RO (43–58%) . At a dose that was efficacious in phase III clinical trials (140 mg PO), telcagepant did not achieve significant RO (4–10%). These results indicate that inhibition of central CGRP-R is not essential for the relief of migraine pain by telcagepant. Further studies with more brain-penetrant CGRP antagonists are required to see if additional anti-migraine efficacy can be gained by achieving high central CGRP RO.

Authorship Contributions

Participated in research design: Hostetler, Sanabria-Bohórquez, Fan, Zeng, Selnick, Bell, Salvatore, Kane, Li, de Groot, Van Hecken, de Hoon, Reynders, Declerq, De Lepeleire, Kennedy, Blanchard, Marcantonio, Sur, Cook, van Laere, Evelhoch

Conducted experiments: Hostetler, Fan, Purcell, Gantert, Riffel, Williams, O'Malley, Miller, Bormans, Van Hecken, Derdelinckx, de Hoon, Reynders, Kennedy, Blanchard, Marcantonio, van Laere.

Contributed new reagents or analytic tools: Selnick, Gallicchio, Bell.

Performed data analysis: Hostetler, Joshi, Sanabria-Bohórquez, Zeng, Riffel, Williams, O'Malley, Li, Kennedy, van Laere.

Wrote or contributed to the writing of the manuscript: Hostetler, Joshi, Salvatore, Hargreaves, de Hoon, Declerq, De Lepeleire, Kennedy, Marcantonio, van Laere, Evelhoch.

References

Amin FM, Asghar MS, Hougaard A, Hansen AE, Larsen VA, de Koning PJH, Larsson HBW, Olesen J, and Ashina M (2013) Magnetic resonance angiography of intracranial and extracranial arteries in patients with spontaneous migraine without aura: a cross-sectional study. *Lancet Neurol* **12**:454–461.

Asghar MS, Hansen AE, Amin FM, van der Geest RJ, Koning Pv, Larsson HBW, Olesen J, and Ashina M (2011) Evidence for a vascular factor in migraine. *Ann Neurol* **69**:635–645.

Bahra A, Matharu MS, Buchel C, Frackowiak RS, and Goadsby PJ (2001) Brainstem activation specific to migraine headache. *Lancet* **357**:1016–1017.

Bell IM, Gallicchio SN, Stump CA, Bruno JG, Fan H, Hostetler E, McWherter M, Moore EL, Mosser SD, Purcell M, Salvatore CA, Sanabria S, Staas DD, White RB Zartman BC, Zeng Z, Cook JJ, Hargreaves R, Kane SA, Graham SL, Selnick HG (2013) Discovery of [^{11}C]MK-4232: the first positron emission tomography tracer for the calcitonin gene-related peptide receptor [published online ahead of print July 18, 2013]. *ACS Med Chem Lett* doi:10.1021/ml400199p.

Bell IM, Gallicchio SN, Wood MR, Quigley AG, Stump CA, Zartman CB, Fay JF, Li CC, Lynch JJ, and Moore EL, et al. (2010) Discovery of MK-3207: A highly potent, orally bioavailable CGRP receptor antagonist. *ACS Med Chem Lett* **1**:24–29.

Borsook D, Moulton EA, Tully S, Schmahmann JD, and Becerra L (2008) Human cerebellar responses to brush and heat stimuli in healthy and neuropathic pain subjects. *Cerebellum* **7**:252–272.

Cunningham VJ and Jones T (1993) Spectral analysis of dynamic PET studies. *J Cereb Blood Flow Metab* **13**:15–23.

Cunningham VJ, Rabiner EA, Slifstein M, Laruelle M, and Gunn RN (2010) Measuring drug occupancy in the absence of a reference region: the Lassen plot revisited. *J Cereb Blood Flow Metab* **30**:46–50.

Dohta Y, Yamashita T, Horiike S, Nakamura T, and Fukami T (2007) A system for LogD screening of 96-well plates using a water-plug aspiration/injection method combined with high-performance liquid chromatography-mass spectrometry. *Anal Chem* **79**:8312–8315.

Grimwood S and Hartig PR (2009) Target site occupancy: emerging generalizations from clinical and preclinical studies. *Pharmacol Ther* **122**:281–301.

Hamill TG, Sato N, Jitsuoka M, Tokita S, Sanabria S, Eng W, Ryan C, Krause S, Takenaga N, and Patel S, et al. (2009) Inverse agonist histamine H3 receptor PET tracers labelled with carbon-11 or fluorine-18. *Synapse* **63**:1122–1132.

Ho AP, Dahlöf CGH, Silberstein SD, Saper JR, Ashina M, Kost JT, Froman S, Leibensperger H, Lines CR, and Ho TW (2010) Randomized, controlled trial of telcagepant over four migraine attacks. *Cephalalgia* **30**:1443–1457.

Ho TW, Ferrari MD, Dodick DW, Galet V, Kost J, Fan XY, Leibensperger H, Froman S, Assaid C, and Lines C, et al. (2008) Efficacy and tolerability of MK-0974 (telcagepant), a new oral antagonist of calcitonin gene-related peptide receptor, compared with zolmitriptan for acute migraine: a randomised, placebo-controlled, parallel-treatment trial. *Lancet* **372**:2115–2123.

Hostetler ED, Hamill T, Francis BE, and Burns HD (2001) A versatile, commercially available automated synthesizer for the development and production of PET radiotracers. *J Labelled Comp Radiopharm* **44**:S1042–S1044.

Inagaki S, Kito S, Kubota Y, Girgis S, Hillyard CJ, and MacIntyre I (1986) Autoradiographic localization of calcitonin gene-related peptide binding sites in human and rat brains. *Brain Res* **374**:287–298.

Innis RB, Cunningham VJ, Delforge J, Fujita M, Gjedde A, Gunn RN, Holden J, Houle S, Huang SC, and Ichise M, et al. (2007) Consensus nomenclature for in vivo imaging of reversibly binding radioligands. *J Cereb Blood Flow Metab* **27**: 1533–1539.

Matthews PM, Rabiner EA, Passchier J, and Gunn RN (2012) Positron emission tomography molecular imaging for drug development. *Br J Clin Pharmacol* **73**: 175–186.

Moulton EA, Schmahmann JD, Becerra L, and Borsook D (2010) The cerebellum and pain: passive integrator or active participator? *Brain Res Brain Res Rev* **65**: 14–27.

Paone DV, Shaw AW, Nguyen DN, Burgey CS, Deng JZ, Kane SA, Koblan KS, Salvatore CA, Mosser SD, and Johnston VK, et al. (2007) Potent, orally bioavailable calcitonin gene-related peptide receptor antagonists for the treatment of migraine: discovery of N-[(3R,6S)-6-(2,3-difluorophenyl)-2-oxo-1- (2,2,2-trifluoroethyl)azepan-3-yl]-4- (2-oxo-2,3-dihydro-1H-imidazo[4,5-b]pyridin- 1-yl)piperidine-1-carboxamide (MK-0974). *J Med Chem* **50**:5564–5567.

Patel S and Gibson R (2008) In vivo site-directed radiotracers: a mini-review. *Nucl Med Biol* **35**:805–815.

Salvatore CA, Hershey JC, Corcoran HA, Fay JF, Johnston VK, Moore EL, Mosser SD, Burgey CS, Paone DV, and Shaw AW, et al. (2008) Pharmacological characterization of MK-0974 [N-[(3R,6S)-6-(2,3-difluorophenyl)-2-oxo-1-(2,2,2-trifluoroethyl)azepan-3-yl]-4-(2-oxo-2,3-dihydro-1H-imidazo[4,5-b]pyridin-1-yl)piperidine-1-carboxamide], a potent and orally active calcitonin gene-related peptide receptor antagonist for the treatment of migraine. *J Pharmacol Exp Ther* **324**:416–421.

Salvatore CA and Kane SA (2011) CGRP receptor antagonists: toward a novel migraine therapy. *Curr Pharm Biotechnol* **12**:1671–1680.

Salvatore CA, Moore EL, Calamari A, Cook JJ, Michener MS, O'Malley S, Miller PJ, Sur C, Williams DL, Jr, and Zeng ZZ, et al. (2010) Pharmacological properties of MK-3207, a potent and orally active calcitonin gene-related peptide receptor antagonist. *J Pharmacol Exp Ther* **333**:152–160.

Tschopp FA, Henke H, Petermann JB, Tobler PH, Janzer R, Hökfelt T, Lundberg JM, Cuello C, and Fischer JA (1985) Calcitonin gene-related peptide and its binding sites in the human central nervous system and pituitary. *Proc Natl Acad Sci USA* **82**:248–252.

Vincent M and Hadjikhani N (2007) The cerebellum and migraine. *Headache* **47**: 820–833.

Weiller C, May A, Limmroth V, Jüptner M, Kaube H, Schayck RV, Coenen HH, and Diener HC (1995) Brain stem activation in spontaneous human migraine attacks. *Nat Med* **1**:658–660.

Yamazaki M, Neway WE, Ohe T, Chen IW, Rowe JF, Hochman JH, Chiba M, and Lin JH (2001) In vitro substrate identification studies for p-glycoprotein-mediated transport: species difference and predictability of in vivo results. *J Pharmacol Exp Ther* **296**:723–735.

Zeng Z, O'Malley S, Miller PJ, Hostetler E, Fan H, Kim J, Selnick H, Wood M, Graham S, Kane S, et al. (2009) A novel radioligand for calcitonin gene-related peptide (CGRP) receptors: In vitro autoradiography and tissue homogenate binding studies, in *2009 Neuroscience Meeting Planner*; 2009 Nov 12-16; Chicago, IL. Program No. 586.17, Society for Neuroscience, Washington, DC.

Address correspondence to: Eric Hostetler, Merck Research Laboratories, WP44D-2, West Point, PA 19486. E-mail: eric_hostetler@merck.com